



Mechanical Stress Analysis of the Lower Link Arm Tractor Connect Paddy Field Sowing Machine Using Finite Element Method

Nattadon Pannucharoenwong¹, Suwipong Hemathulin^{2,*}, Thodsatam Lasopha², Phadungsak Rattanadecho¹, Jirawadee Polprasert³, and Penpimol Luekhajorn⁴

ARTICLE INFO

Article history:

Received: 17 May 2021

Revised: 21 June 2021

Accepted: 5 October 2021

Keywords:

Lower link arm,

Paddy field sowing machine

Static analysis,

Finite element method

ABSTRACT

The objective of this research paper is to investigate the mechanical stress of the tractor lower hitch system when attaching the grain sowing equipment using finite element method and creating a three-dimensional model of the tractor's extension arm system. There are two types of lower peripheral arms, type A and type B. The maximum load conditions are 700 kg when the weight of the peripheral equipment is included. The pull force was analyzed based on static principle and fatigue of the lower peripheral arm system. The results of the analysis showed that the maximum stress of the lower arm B at the peripheral point of the sowing machine was 150.47 MPa, while the von-miss stress of lower arm A was distinct at 104.37 MPa. The safety factor (FS) of the lower arm A was 1.57 while the safety factor of the lower arm B was 1.54 which is a difference of 3.09%. Fatigue analysis of lower arm A revealed a fatigue value of 124.67 MPa and for lower arm B the fatigue value was 179.97, which is a difference of 44.36%. In the actual test, 1rai of rice seed test took 1 hour with engine speed 1500 rpm to complete. The 1st gear was used to test the results. The horizontal force acting on the lower arm A is 3100 N and the lower arm B is 3400 N, which is a difference of 8.82%. These results show that the lower arm A has less force, higher safety factor (FS), and less fatigue than the lower arm B. The force acting on the lower arm A in this experiment was relatively lower compared with results from other researches, which suggested that lower arm A have appropriate strength and it is suitable for use in actual agricultural work.

1. INTRODUCTION

Thailand's agricultural sector has long played an important role in Thailand's economy and job creation. The agricultural occupation of Thai farmers has changed completely from the past. New technologies are introduced to help save labor and increase production capacity for Thai farmers in many areas that are engaged in commercial agriculture. The trend of using agricultural machinery in Thailand has skyrocketed. One of the major problems in Thai agriculture is that there is a shortage of agricultural labor. Therefore, agricultural machinery, labor-saving, must be used in solving the problem effectively on the spot. Adopting agricultural machinery that is both technological and efficient in agriculture is a key factor in expanding production capacity, reduce production costs and reduce the time of cultivation which will help increase the yield efficiency. Agricultural machinery for pre-harvesting such as tractors, plows, rice cultivators are becoming popular in the Isan region because the grain can be sown quickly and efficiently which reduce the labor for farming and reduce the

cost of rice production as well.

Efforts have been made to continuously study and improve agricultural machinery efficiency by studying factors such as stress distribution, deformation, enhancement of components, and computer-aided structural design to suit the local environment and terrain [1] - [3].

Analysis using Finite Element Method (FEM) methodology is now popular and analytical accuracy, reliable and can be employed to calculate the shape, stress, strain and deformation of the mechanical parts and identify the critical points that would occur before the actual mechanical prototyping [4] - [6]. Optimization using finite element method. (FEM) can be performed quickly and easily by changing properties that affect performance such as arterial type and surface condition This method leads to analysis in a virtual environment without the need for actual prototyping to obtain a complete and optimal prototype [7] - [9].

¹Department of Mechanical Engineering, Thammasat University, Pathumthani, 12120, Thailand.

²Department of Mechanical and Industrial Rajabhat Sakon Nakhon University 47000, Thailand.

³Department of Electrical and Computer Engineering, Naresuan University, 65000, Thailand.

⁴PTS Combination Co.,Ltd, 315/116 Moo 3, Ban Mai, Pakkret, Nonthaburi 11120, Thailand.

*Corresponding author: S. Hemathulin; Phone+66 0935519414; E-mail: suwipong@sru.ac.th.

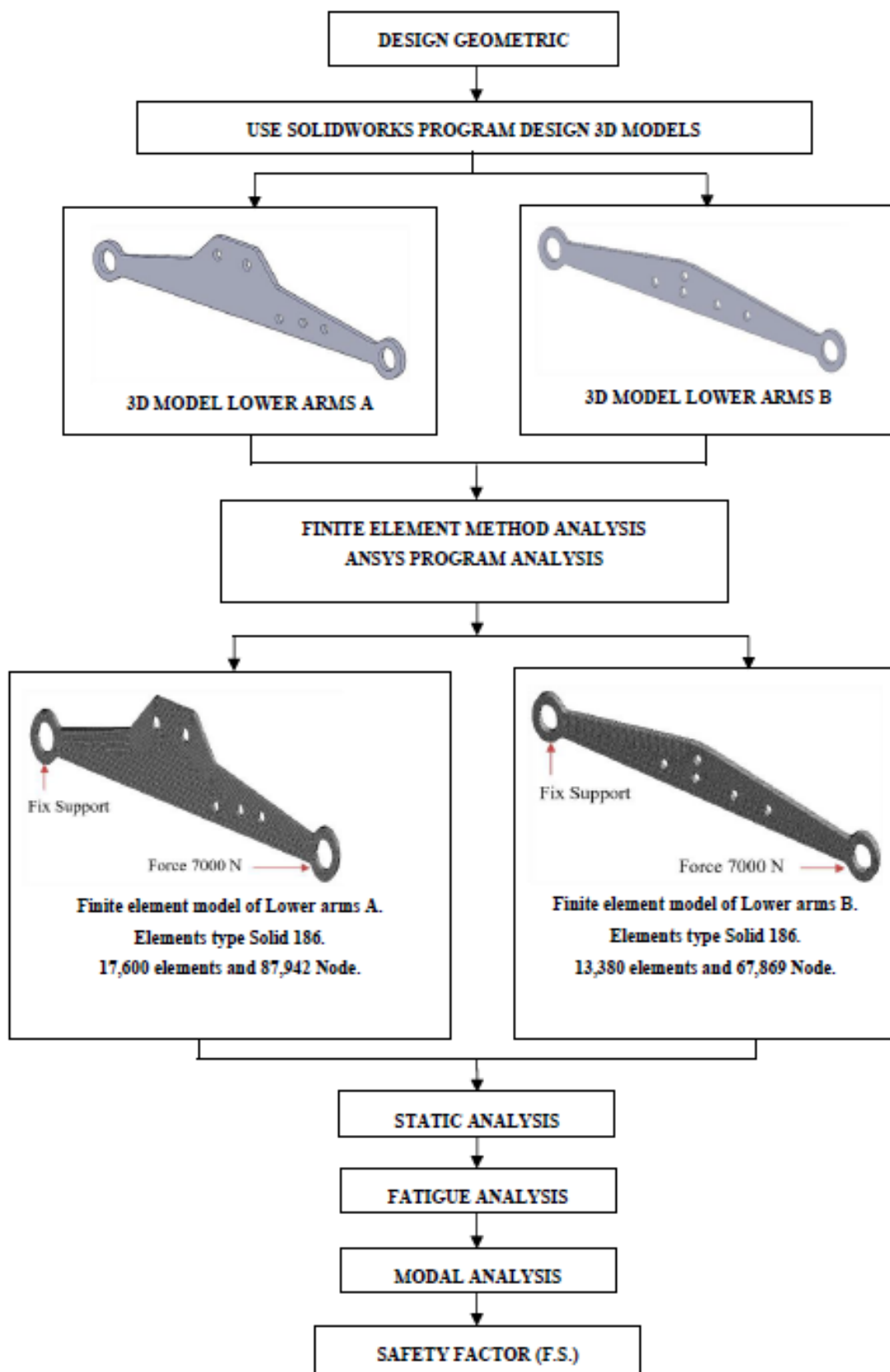


Fig.1. Flow chart design 3D models and finite element method analysis

Agricultural machinery has a large number of moving parts and operates under sustained and large dynamic loads that can cause damage and stop working. Several studies have been undertaken to study the behavior of agricultural machinery [10] using finite element method for study and analysis. Tiller tractors are very popular agricultural machinery in Thailand. It is used for plowing, lifting, and retrieving peripherals such as the dry rice seeder, which is gaining popularity as a timesaving, convenient, quick and efficient farming aid [11]. One of the major problems with the tiller is that when it is damaged or deformed of the lower tiller arm or the lower part of the lower hinge assembly because of its high load. Therefore, the lower extension arm is an essential part of the tractor to attach equipment and the damage of this equipment when it occurs will affect other peripherals. As a result, the damage is widespread and farmers can sometimes be injured.

Therefore, it is imperative to analyze the mechanical load of the tractor lower limb under realistic operating conditions [12]. This study aimed to analyze and simulate the mechanical stress exerted on the tractor's lower peripheral arm system when attaching the grain sowing machine. The finite element method was used to analyze static force, fatigue of the lower peripheral arm system and analyzes the maximum von-miss stress that occurs. These values influence the sizing and configuration of the lower peripheral arms to suit them when applied to the peripheral of the rice seeder in the field for real testing.

2. DESIGN AND EXPERIMENTAL

2.1 Design geometric

Experimental procedure flow chart is shown in Fig. 1. The experimental design created a 3D model of the tractor lower tiller system to determine the experimental distance in the real environment as shown in Fig. 2. The whole system as shown in Table 1. By defining the conditions in the design assistant to create a 3D model in order to obtain the analysis results as close as possible to the actual working conditions.

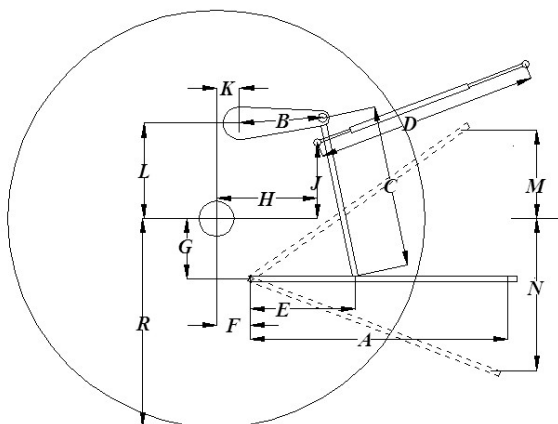


Fig. 2 . Details of-3 point hitch linkage system [13].

Given parameters.

- A = Distance link.
- B = Distance lift arm.
- C = Distance lift rod.
- D = Distance upper link.
- E = Distance lift rod connection.
- F = Distance pivot point of lower link from the rear wheel (horizontal oriented).
- G = Distance pivot point of lower link from the rear wheel axle center (vertical oriented).
- H = Distance pivot point of upper link from the rear wheel axle center (horizontal oriented).
- J = Distance pivot points of upper link from the rear wheel axle center (vertical oriented).
- K = Distance pivot points of lift arm from the rear wheel axle center (horizontal oriented).
- L = Distance pivot points of lift arm from the rear wheel axle center (vertical oriented).
- M = Maximum length height from the center of rear wheel axle.
- N = Minimum length height from the center of rear wheel axle center to the lower hitch location.
- R = Distance dynamic radius tractor's rear wheel.

Design the lower tractor extension arm by designing it using SolidWorks 3D design assistant to create a model of the lower trailer arm. The design of the lower extension arm A as shown in Fig. 3. and the lower extension arm type B as shown in Fig. 4. Then the model is converted to Iges files to enter the finite method analysis Ansys program to help in the analysis. The material properties of the lower extension arm are steel (St 37) [14] as shown in Table 2. The model of the lower extension arm is installed at the rear of the tractor as shown in Figure 5.

Table 1. Determine the testing phase of the tractor of 3-point hitch linkage system [13].

Name	Dimension (mm)	Setting test (mm)
A	730	730
B	235	235
C	415 to 465	465
D	533 to 630	630
E	300	300
F	95	95
G	170	170
H	280, 285, 270	285
J	215, 245, 285	245
K	65	65
L	270	270
M	250 to 350	250
N	290 to 430	430
R	590	590

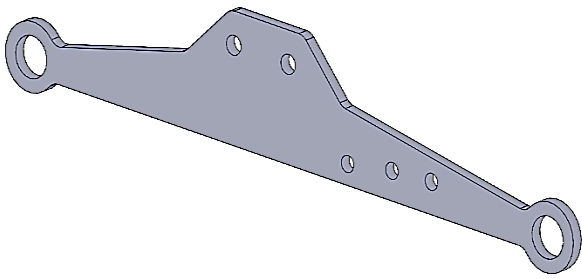


Fig. 3. Lower arms A.

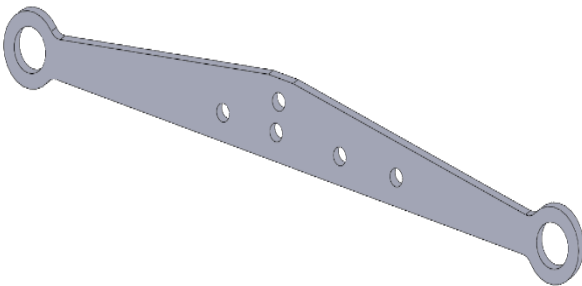


Fig. 4. Lower arms B.

Table 2. Mechanical properties of steel (St 37)

Density, σ (kg/m ³)	Modulus of elasticity, E (GPa)	Poisson's ratio, ν	Yield strength, σ_{yp} (MPa)	Ultimate tensile strength, σ_{ut} (MPa)
7860	200	0.3	198	235



Fig. 6. installation lower link arms 3D Models.



Fig. 7. installation lower link arms and equipment paddy field sowing machine.



Fig. 5. Installation area of the lower extension arm to the tractor.

And before the actual creation has design lower link arms to connected paddy field sowing machine and installation area of the lower link arms shown in Fig. 6. All equipment was built and installed into the tractor body for testing in the prepared test plot shown in Fig. 7.

2.2 Calculation of lift arm's power

Hitch linkage system can be analyzed in term of kinematic considering the tractor rear axle's center as the point of origin. The total distance between the hitch point and lift arm equaled $M + N$ is shown to result in full power as demonstrated in Fig.2 and Fig. 8. When the carried weight is vertical and the lower link is located horizontally then the angle parameters as shown in Fig.8 are as follow: $\varphi_2= 3 \pi / 2$ radians, $\varphi_3= \pi$ radians and $\alpha = \pi / 2$ radians. Some value such as θ and φ_1 can be found by geometry of the setup. The coordinates' location of lower hitch points can be calculated using the following equation.

$$x_A = K + B \sin \theta + C \sin \varphi_1 + (A - E)(\varphi_2 - \pi) \quad (1)$$

$$y_A = L - B \cos \theta - C \cos \varphi_1 - (A - E) \sin(\varphi_2 - \pi) \quad (2)$$

The value of θ was depicted as θ level which increased in small increment after a certain value of force is applied on the experimental setup. Summation of vertical and horizontal force component in the form of vector for the first four-bar linkage along with different defining function (f_1 and f_2) and B, C, E and Q as shown in Fig. 8. The equations related to Fig.8 can be described as follow:

$$F.S.=\frac{\sigma_{yp}}{\sigma_{all}} \tag{5}$$

3.2 Fatigue analysis

The impact of the load on the tractor's coupling arms repeatedly (cyclic loads) causes cracks, while the reversal of the stress is less than the yield stress (yield stress) of the tractor lower peripheral arm structure, and eventually a fracture caused by the fatigue of the tractor lower limb system, the equation to calculate the mean stress arising. This is shown in Equation (6) by calculating the safety factor (F.S.), which is obtained from Soderberg's equation [17] as shown in Equations (7) and (8).

$$\sigma_{all}=\frac{\sigma_{max}-\sigma_{min}}{2} \tag{6}$$

$$\frac{1}{F.S.}=\frac{\sigma_{ave}}{\sigma_y}+K\frac{\sigma_r}{\sigma_e} \tag{7}$$

$$\sigma_r=\frac{\sigma_{max}-\sigma_{min}}{2} \tag{8}$$

3.3 Modal analysis

The natural frequency of the tractor lower limb structure depends on the shape, design and material being built, as well as the load point of the tractor. The amount and type of force exerted will affect the natural frequency. Modal analysis with finite element method can predict the design of tractor lower hitch system and natural frequency. The equations involved in the analysis are Equation (9) and Equation (10) [18] and modal analysis is essential in the design of parts and structures because deformation can be predicted and may also occur in a designed structure. In this experiment, modal analysis of the tractor lower trailer arm was performed using 5 natural frequencies with a frequency range of 0- 5,000 Hz.

$$[M]\{\ddot{u}\}+[C]\{\dot{u}\}+[K]\{u\}=\{F(t)\} \tag{9}$$

$$(-\omega_i^2[M]+[K])\{u\}=0 \tag{10}$$

4. EXPERIMENTAL SETUP

Components of the dry rice seeder are shown in Fig.12 [11]. The dimension of the dry rice seeder is 150 cm x 120 cm x 100 cm. Components 1 represent seed box for storing rice seeds, 2. fertilizer box used for collecting fertilizer, 3. rice seed swivel disc used for conveying grain, 4. toolbar frame of the sowing machine, 5. seed delivery tube for conveying seeds into the sowing hole and 6. depth control bar to adjust the depth of sowing of rice. Abbreviations should be clearly defined on first occurrence and should be used consistently throughout the text. Detailed mathematical discussion should be placed in an appendix.

Vertical grain spinning discs are installed as shown in Fig.13. All equipment are connected to a 24 hp tractor which is capable of sowing 7 rows of seed at a time. Actual testing was performed at Tan Kon Village, Sawang Daen Din District, Sakon Nakhon Province. The field (1 rai) consisted rice varieties including Khao Dok Mali 105 which was used for this research. Before the seed sowing test, soil must be prepared in the field to be used for testing by plowing and breaking the soil. The test took 5 hours, used all 5 liters of diesel fuel, the grain pitch of 25 cm x 25 cm, and the engine speed was set to 1,500 rpm [19]. The two different type of lower link arms (A and B) were installed and the results were monitored and recorded using the MT-250D storage device shown in Fig. 14.

The position of the Force sensor device is located on the tractor extension arm. It is installed at the upper arm 1 point and the left and right arm 1 point on each side [19] as shown in Fig. 15. Afterward the results were compared with another research, summarized and shown in Table 3.

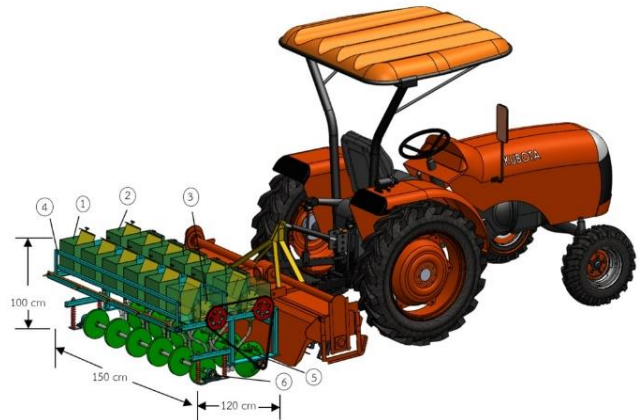


Fig. 12. Dry paddy field sowing machine part specification. 1. seed box, 2. fertilizer box, 3. rice seed swivel disc, 4. toolbar frame, 5. seed delivery tube, 6. depth control bar [11].



Fig. 13. Vertical seed swivels disc with sowing machine.



Fig. 14. Data MT-250D and acquisition system.

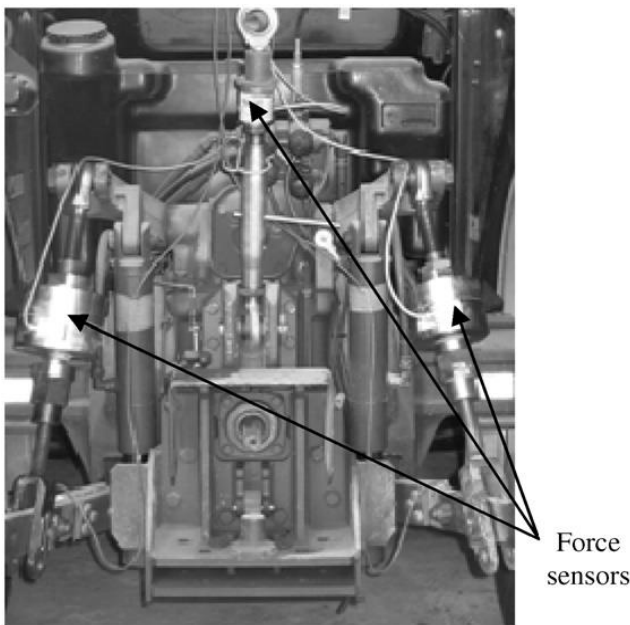


Fig. 15. Installation force sensors area.

Table 3. Experimental condition

Test condition	
1. Total area	1 Rai
2. Time to test	1 Hour
3. Total fuel	5 Liter
4. Engine speed	1500 rpm
5. Gear ratio	1
6. Weight	700 Kilogram

5. RESULT AND DISCUSSION

5.1 Result static analysis

From the analysis of the stress distribution using finite element method, it was determined that the properties of

material SOLID 186, which is the real property of the steel that will be used to construct this workpiece. The actuated load was 700 kg, equal to the weight of the actual rice seeder analyzed by the Ansys program of the tractor lower trailer arm type A lower attachment point of the extension arm. The resulting stress value is 104.37 MPa, which is the point where it is connected to the grain sowing machine as shown in Fig. 16. The safety factor (FS) calculated from Equation (1) is equals 2.00.



Fig. 16. Von- Mises stress on lower link arm A.

As for the lower coupling arm system of tractor type B, the maximum stress Von-Mises occur at the lower end of the coupling, as with Type A, the resulting stress is 150.47 MPa, which is greater than the lower hitch types A and is the point to be connected to the grain sowing machine. This result is similar to the type A lower hitch which occurs nearby as shown in Fig. 17 and Safety Factor calculated from equation (1) was 1.94, which is less than the type A system. Additionally, the lower limb system deformation analysis data of the tractor models A and B are shown in Table 3.

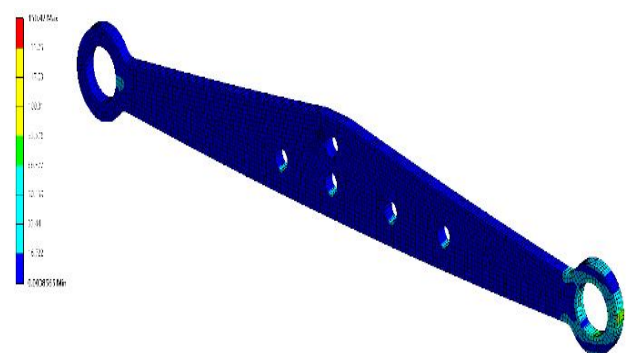


Fig. 17. Von- Mises stress on lower link arm B.

The effect of Von-Mises on the type A-lower peripheral arm was compared with type B and compared with the previous research [14] shown in Fig. 18. The lower arms type A demonstrated the least Von-mises stress and the stress value of the lower arms type B is the largest. This may

be due to the material properties of the peripheral equipment and the specified environment that is use to conduct the simulation. The stress value of Lower arms B is 6.38% higher compared with the stress value of the lower arms MF285. In terms of the safety factor (FS)), the lower arms type A demonstrated a maximum value of 2.00 and the lower arms type B has a value of 1.95, lower arms MF399 has a value of 1.45 and lower arms MF285 has a value of 1.40, shown in Fig. 19. Different values are related to the material properties and the position of the workpiece design, which affects the accuracy and safety of the lower extension arm.

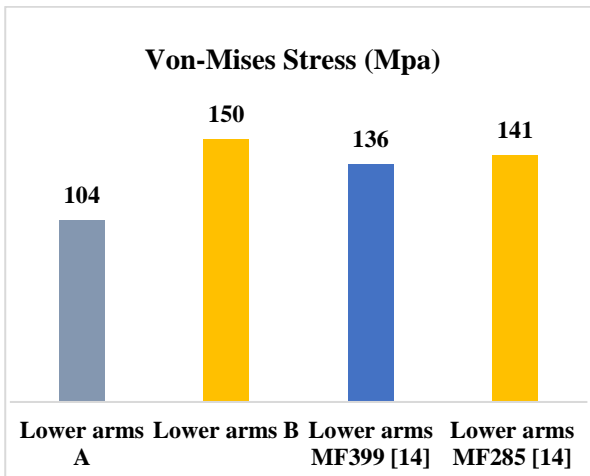


Fig. 18. Compare Von-Mises Stress.

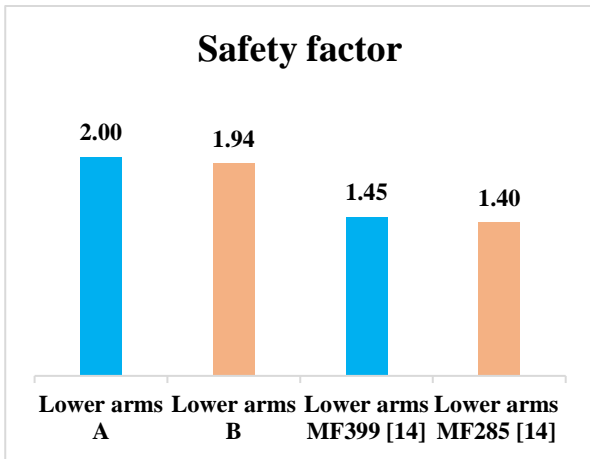


Fig. 19. Compare Safety factor (F.S.).

Table 4. Deformation of the tractor lower trailer arm

Peripheral device	Deformation(mm)	
	Lower extension arm A	Lower extension arm B
Rice seeder	0.24304	0.36026

From Table 4, the maximum deformation occurring with A-type lower arm was 0.24304 mm, which is lower than that of type B lower arm at 0.36026 mm.

The results of static analysis with this finite element method show that most of the stress occurs at the junction of the rice seeder. This makes this area the most vulnerable to fracture.

5.2 Result fatigue analysis

In the analysis of fatigue by finite element method, it is necessary to determine the conditions of the force that are acting as realistically as possible so that the analysis results are reliable. The fatigue analysis will need to be conducted using repetitive stress for the tractor lower trailer arm system. This analysis set the stress limit at 1.9 million cycles [20], [21]. Test results indicated the maximum fatigue occurring on the tractor-type A lower arm system, 124.67 MPa. Another point occurred at the end of the lower coupling arm, which is the area to be connected to the sowing machine is shown in Fig. 20. And the safety factor occurring at the junction end of the lower peripheral arm is 1.57 as shown in Fig. 21.

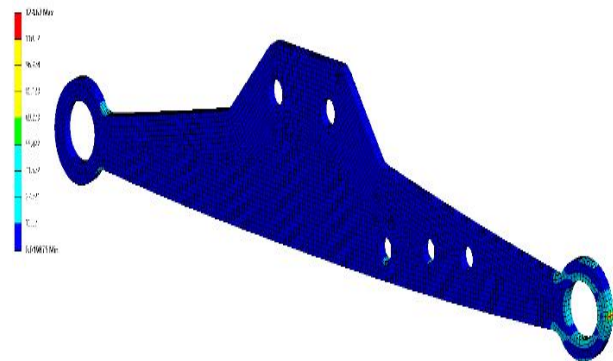


Fig. 20. Fatigue on Lower arms A

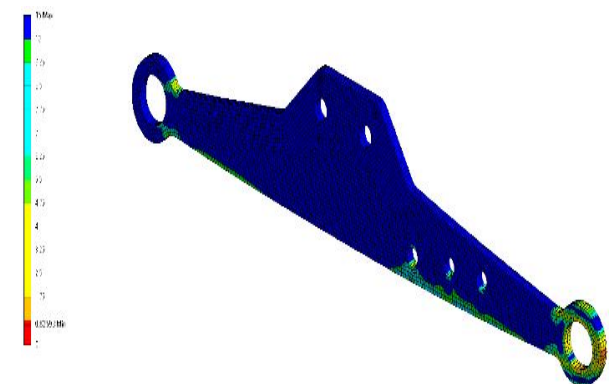


Fig. 21. Safety factor (F.S.) on lower link arm A.

As for the fatigue occurring on the lower trailer arm, type B tractor the value resulted was 179.97 MPa. The fatigue occurred at the end of the lower tonnage arm which was the

area to be connected to the grain sowing machine, as shown in Fig. 22. And the safety factor occurring at the junction end of the lower peripheral arm is 1.54 shown in Fig. 23.

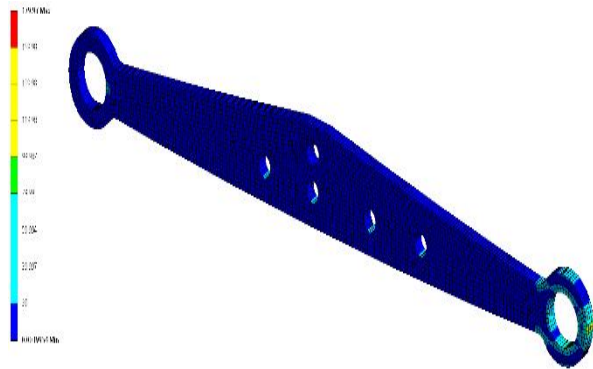


Fig. 22. Fatigue on Lower arms B

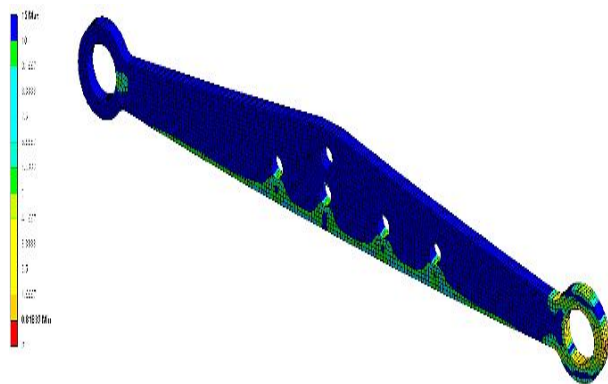


Fig. 23. Safety factor (F.S.) on lower link arm A.

The fatigue of the lower arms A, which was 124.67 MPa, and the fatigue of the lower arms B, which was 179.97 MPa are compared with previous research [14] as shown in Fig. 24. Lower arms A demonstrated the least fatigue, whereas the lower arms B demonstrated the largest fatigue. This indicates the damage that can occur to the lower arms B is the most damaging at the peripheral connection points and at the levelling borehole. The safety factor is shown in Fig. 25. The safety value of the lower arms A has a value of 1.57, Lower arms B has a value of 1.54, in the lower arms MF399 has a value of 1.55 and the lower arms MF285 has a value of 1.56, which are very similar to each other.

5.3 Result modal analysis

The modal analysis results are shown in Table 4 it can be seen that with increasing the number of natural frequencies in the experiment, the frequency of both the A and B tractor lower limbs increased, respectively. However, considering Table 5 it was found that the frequency values of Type B lower arm structures were higher than Type A, which makes it possible to predict that the type B lower peripheral structures are more likely to damage than those of type A.

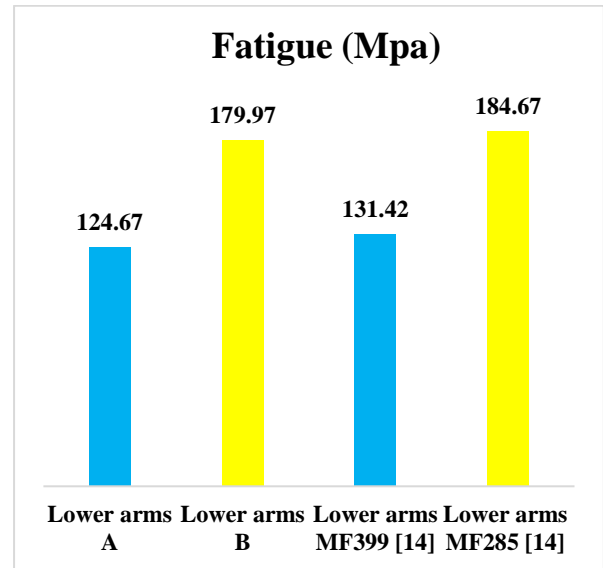


Fig. 24. Compare fatigue

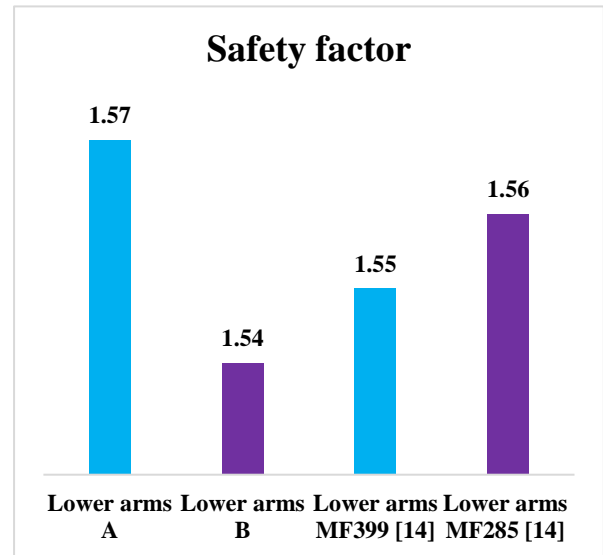


Fig. 25 Compare Safety factor (F.S.)

Table 5. Natural frequency of tractor lower link arm frequency range (0-5,000 Hz)

Frequency number	Frequency) Hz)	
	Lower extension arm A	Lower extension arm B
1	15.432	15.393
2	52.846	51.34
3	85.925	92.466
4	197.07	259.02
5	261.32	312.36

5.4 Result experimental

Fig. 26 demonstrated the experimental forces was shown by measuring the horizontal force exerted on both the A and B peripheral arms, comparing the results with previous studies. [20]. The results of the experiment showed that the forces acting on the lower limb horizontally had similar forces comparable to other research. The force acting on the lower arm A is minimal, the mean is 3100 N and the force acting on the lower arm B increases, to 3400 N. The working force of the research carried out on the engine system is compared with data from other research with an average force of 4100 N.

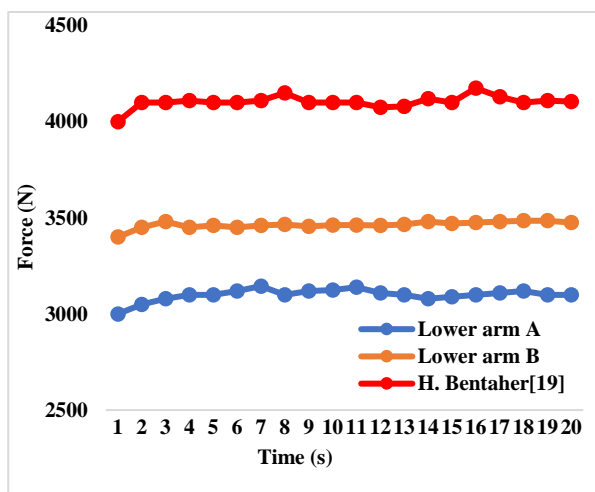


Fig. 26. Compare experimental force on lower link arm.

6. CONCLUSION

The finite element method analyzed in this research was able to analyzed the stress and dispersion as well as the deformation of tractor lower trailer arm parts by the Von-Misses on the extension arm. Tractor A has a value of 104.37 MPa, and the Von-misses stress with a tractor B tractor is 150.47 MPa. In comparison, the safety factor (FS) found that the type A lower arm was 3.09% higher than the type B lower arm at 3.09%. Fatigue of type A was 124.67 MPa, type B lower limb had fatigue 179.97 MPa, fatigue of type B was 44.36% higher than type A. When comparing the safety factor (FS), it was found that the result of modal analysis when increasing the number of natural frequencies from 1 - 5 was found that at the 5th natural frequency, type B lower limb had frequency that is 19.53% higher than the lower arm types A, which is the design trend of the extension arm. We can summarize the results from the analysis with the finite element method and the safety factor (FS) that occurred, showing that the design of the tractor lower trailer arm system A when the seeder is attached is stronger and result in lower damaged than that of the bottom type B lower arm when the seeder is attached.

In the area of the experiment, it was found that the force acting horizontally on the lower arm A was averaged at 3100N and the force acting on the lower arm B was averaged

at 3400N. The force acting on the lower arm A was 300 N which was 8.82% lower compared with lower arm B. The averaged force of 4100N acting on the lower arm is 24.39% lower than results from other researches. This indicated that the lower arm A should be chosen because it has less force on the workpiece. The damage to the workpiece is therefore less likely to be noticeable and is consistent with the analysis of finite element method. This shows that the lower arm A has less stress, lower fatigue and a higher safety factor than the lower arm B.

ACKNOWLEDGMENT

This research was supported by Research Fund from Thammasat School of Engineering, Faculty of Engineering, Thammasat University. This research would like to thank the farming center of Tan Khon Village, Tan Kone Subdistrict, Sawang Daen Din District, Sakon Nakhon Province for providing assistance or testing and supported facilities as well as reporting problems arising from application until the research was successful. Additionally, the authors would like to acknowledge Faculty of Industrial Technology and Rajabhat Sakon Nakhon University that provides support throughout the research project.

NOMENCLATURE

- α Angle between vertical reference time and the lower link.
- β Angle between lift arm and pivot points of lower link.
- θ Angle between vertical reference line and lift arm.
- φ_1 Angle between vertical reference line and lift rod.
- φ_2 Angle between vertical reference time and lower link.
- φ_3 Angle between weight and the vertical reference line. references list.

REFERENCES

- [1] Kalpakjian, S. and Schmid, S.R. (2001). *Manufacturing Engineering and Technology 4th*, Prentice-Hal Inc., Upper Saddle River.
- [2] Jahanbakhshi, A., Ghamari, B., and Heidarbeigi, K. (2016). Effect of engine rotation speed and gear ratio on the acoustic emission of John Deere 1055I combine harvester. *Agric. Eng. Int. CIGR J.* 18(3), pp. 106 – 112.
- [3] Jahanbakhshi, A., Ghamari, B., and Heidarbeigi, K. (2017). Assessing acoustic emission in 1055I John Deere combine harvester using statistical and artificial intelligence methods, *Int. J. Veh. Noise Vib.* 13(2), pp. 105 – 117.
- [4] Jahanbakhshi, A., Heidari Raz Darreh, S., and Kheiralipour, K. (2018). Simulation and static and fatigue analysis of cross bar of moldboard plough by finite element method (FEM), *Iran. J. Biosyst. Eng.* 49(3), pp. 341 – 352
- [5] Ryken, M.J. and Vance, J.M. (2000). Applying virtual reality techniques to the interactive stress analysis of a tractor lift

- arm, *Finite Elem. Anal. Des.* 35, pp. 141 – 155.
- [6] Seyedabadi, E. (2015). Finite element analysis of lift arm of a MF-285 tractor three-point hitch, *J. Fail. Anal. Prev.* 15(5), pp. 737 – 743.
- [7] [7] Mirehei, A., Hedayati Zadeh, M., Jafari, A. and Omid, M. (2008). Fatigue analysis of connecting rod of universal tractor through finite element method (ANSYS), *J. Agric. Technol.* 4(2), pp. 21 – 27.
- [8] Lo, S.H.R. and Bevan, A. (2002). Fatigue analysis of a plate-with-a-hole specimen and a truck exhaust bracket using computer-based approach. *Int. J. Eng. Simul.* 4(2), pp. 61 – 69.
- [9] R, Alimardani., Z, Fazel., A, Akram., A, Mahmoudi., and M, G, Varnamkhasti. (2008). Design and Development of a three-point hitch dynamometer. *Journal of Agricultural Technology.* 4(1), pp. 37 – 52.
- [10] Mouazen, A.M. and Nemenyi, M. (2000). Finite element analysis of subsoil cutting in non-homogeneous sandy loam soil. *J. Soil Tillage Res.* 151, pp. 1 – 15.
- [11] Hemathulin, S., Lasopha, T., Pannucharoenwong, N., Rattanadecho, P. and Echaroj, S. (2019). Effect of the orientation of the rice seed swivel disc on the seed consumption rate of the dry paddy field sowing machine, *Journal of Research and Applications in Mechanical Engineering*, Vol. 7, No. 2, pp. 112 – 121.
- [12] S. S. Ambike and J. P. Schmiedeler. (2007). Application of geometric constraint programming to the kinematics design of three-point hitches, *Applied Engineering in Agriculture*, Vol. 23(1), pp. 13-21.
- [13] Prasanna Kumar G.V. (2015). Geometric performance parameters of three - point hitch linkage system of a 2WD Indian tractor, *Res. Agr. Eng.* 61, pp. 47 – 53.
- [14] Ahmad, J. and Kobra, H. (2019). Simulation and Mechanical Stress Analysis of the Lower Link Arm of a Tractor Using Finite Element Method, *J Fail. Anal. and Preven.* 19, pp. 1666 – 1672.
- [15] Kumar G.V.P. (2012). Development of a computer program for the path generation of tractor hitch points. *Biosystems Engineering.* 113, pp. 272–283.
- [16] Budynas, R.G. and Nisbett, J.K. (2011). *Shigley's Mechanical Engineering Design, 9th edn, McGraw-Hill Publisher*, New York.
- [17] Shigley, J.E. and Mischke, C.R. (1989). *Mechanical Engineering Design*, McGraw-Hill Publisher, New York.
- [18] He, J. and Fu, Z.F. (2001). *Modal Analysis, Elsevier*, Amsterdam, pp. 1 – 11.
- [19] H, Bentaher., E, Hamza., G, Kantchev., A, Maalej. And W, Arnold. (2008). Three-point hitch-mechanism instrumentation for tillage power optimization. *BIOSYSTEMS ENGINEERING* 100 (2008), pp. 24–30.
- [20] Cupera, J., Bauer, F., Severa, L. and Tatíček, M., (2011). Analysis of force effects measured in the tractor three-point linkage. *Res. Agric. Eng.* 57, pp. 79 – 87.
- [21] H.F. Al-Jalil, (2012). Design and performance of an adjustable three-point hitch dynamometer, *Soil and Tillage Research*, vol 62, Issues 3-4, pp. 30 - 34.